Supplementary Information and Figures

IL-33 -induced Reactive Oxygen Species is Required for optimal Metabolic Program in Group 2 Innate Lymphoid cells

Authors and affiliations:

Chaoyue Zheng,[a] Haisi Wu,[a, b] Zhen Lu,[a, b] Jiacheng Bi,[a, b, *] Xiaochun Wan[a, b, *]

[a] Shenzhen Laboratory of Fully Human Antibody Engineering, Institute ofBiomedicine and Biotechnology, Shenzhen Institutes of Advanced Technology, Chinese Academy of Sciences,Shenzhen 518055, People's Republic of China

[b] University of Chinese Academy of Sciences, Beijing, People's Republic of China

*Correspondence should be addressed to Xiaochun Wan (xc.wan@siat.ac.cn), or to Jiacheng Bi (jc.bi@siat.ac.cn).

SUPPLEMENTARY METHODS

Mice

C57BL/6 wild-type mice were purchased from Beijing Vital River Laboratory Animal Technology (Beijing, China), or from Hunan SJA Laboratory Animal (Hunan, China). *Nox2*$^{-/-}$ mice and *St2*$^{-/-}$ mice were purchased from Cyagen Biosciences (Jiangsu, China). *Rag1*$^{-/-}$ mice were obtained from the Model Animal Research Center (Jiangsu, China). All mice used were 5 to 8 weeks old, and housed in the specific pathogenfree facility at the Shenzhen Institutes of Advanced Technology, Chinese Academy of Sciences. All animal experiments were approved by the Institutional Animal Care and Use Committee.

Mouse models

For the model of IL-33 –driven ILC2 infiltration into the liver, hydrodynamic injection of 6 μg IL-33 –encoding plasmid was performed to induce IL-33 overexpression in the liver. Mice were i.p. injected with 5 mg NAC / 400 μL PBS, or

25 μg Rapamycin / 5 μL DMSO in 400 μL PBS 6 hour later, and for the next 3 days. Liver lymphocytes were isolated and analyzed 1 day after the final injection.

To induce airway inflammation, we intranasally administered mice with 1μg mouse IL-33 recombinant protein (R&D Systems, MN, USA) every day for four days, and sacrificed these mice one day after the final administration. 5 mg NAC / 400 μL PBS, or 25 μg Rapamycin / 5 μL DMSO in 400 μL PBS was i.p. injected 6 hour after IL-33 administration every day. 1 mL BALF or the lung tissue was harvested for analysis of ILC2 numbers, eosinophil numbers, or cytokine levels.

For the ILC2s adoptive transfer model, 0.5-1 million in vitro expanded mouse ILC2s were i.p. injected into recipient NDG (which lacks ILC2s) or *St2*$^{-/-}$ mice. Two hour after transfer, 5 mg NAC per mice in 0.2 mL PBS or 0.2 mL PBS only was subsequently injected intraperitoneally. Another two hour later,1 μg mouse IL-33 (R&D Systems, MN, USA) in 0.2 mL PBS was injected intraperitoneally. The injection of NAC/PBS and IL-33 was performedfor 4 consecutive days. One day after the last injection, 1 mL peritoneal lavage fluid was collected for ILC2 or eosinophil numbers analysis.

Human PBMCs Preparation

Isolation of human peripheral blood from healthy volunteers was performed by gradientcentrifugation with GE Healthcare Ficoll-Paque™ PLUS Media (Thermo Fisher Scientific, MA, USA). The Ethic Committee of Shenzhen Institute of Advanced Technology approved the experiments.

Cytokine Levels Assessment

Cytokine levels were determined by following kits from BD Biosciences (CA, USA): Mouse/Rat Soluble Protein Master Buffer Kit, Human Soluble Protein Master Buffer Kit, mouse IL-5 Flex Set, mouse IL-13 Flex Set, human IL-5 Flex Set, and human IL-13 Flex Set.

In vitro ILC2s culture and treatment

To obtain mouse ILC2s, murine hepatic lymphocytes from the livers harvested from mice hydrodynamically injected with pcDNA3.1-mcIL-33 plasmid were collected for staining of ILC2 markers and sorting. Freshly sorted mouse ILC2s were expanded in RPMI 1640 complete medium with mouse IL-2, IL-7 (Peprotech, NJ, USA), and IL-33 (R&D Systems, MN, USA). Freshly sorted human ILC2s from peripheral blood were expanded in RPMI 1640 complete medium with human IL-2 (Peprotech, NJ, USA) and IL-33 (R&D Systems, MN, USA). RPMI 1640 complete medium contained 10% fetal bovine serum and 1% Penicillin-Streptomycin solution. Cells were rested for 5-7 days without IL-33 stimulation before re-seeded at 2000 cells/well at round -bottom plate for experiments. In some experiments, final concentration of 5mmol/L NAC (Sigma-Aldrich, MO, USA) was added 2 hour before stimulation with a final concentration of 20ng/ml IL-2, 20ng/ml IL-7, and 5ng/mL IL-33.

Flow cytometryand Sorting

The following fluorescent antibodies were used for flow cytometry:FITC anti-human CD127 (A019D5), FITC anti-mouse/human KLRG1 (2F1/KLRG1), FITC anti-mouse Ly-6G/Ly-6C (Gr-1) antibody (RB6-8C5), PE anti-mouse Ki67 (16A8), PE anti-mouse Lineage Cocktail (145-2C11, RB6-8C5, M1/70, RA3-6B2, Ter-119), PE anti-mouse/human CD11b (M1/70), PE anti-mouse CD98 (RL388), PE anti-mouse CD71 (RI7217), PerCP/Cy5.5 anti-mouse CD90.2 (30-H12), PerCP/Cyanine5.5 anti-human CD294 (BM16), PerCP/Cy5.5 anti-mouse CD11c (N418), APC anti-mouse IL-33Rα (DIH9), APC anti-human CD45 (HI30), APC anti-human Lineage Cocktail (CD3, CD14, CD16, CD19, CD20, CD56) (UCHT1, HCD14, 3G8, HIB19, 2H7, HCD56), eFluor 660 anti-mouse CD170 (eBioscience, 1RNM44N)， Brilliant Violet 510 anti-mouse CD45 (30-F11), PE anti-mouse AKT (pT308) (BD Biosciences, J1-223.371), PE anti-mouse S6 (pS235/pS236) (BD Biosciences, N7-548), Alexa Fluor 647 anti-mouse AKT (pS473) (BD Biosciences, M89-61), Alexa Fluor 647 anti-mouse mTOR (pS2448) (BD Biosciences, O21-404). All antibodies were purchased from Biolegend,unless specified otherwise.

For surface staining, a LIVE/DEAD Fixable Violet Dead Cell Stain Kit (Life Technologies, MA, USA) was used for staining dead cells, before subsequent Fc blocking, and antibody staining. For intracellular staining, a True-Nuclear Transcription Factor Buffer Set (Biolegend, CA, USA) was used to fix and permeabilize cells according to the manufacturer's instructions. CountBright Absolute Counting Beads (Thermo Fisher Scientific, MA, USA) was used for cell counting. Mouse ILC2s were identified as live $CD45^{+}Lineage^{-}ST2^{+}CD90^{+}KLRG1^{+}$ cells (Fig S1, A). Mouse eosinophils were identified as live $CD45^{+}Gr\text{-}1^{+}CD11b^{+}CD11c^{-}CD170^{+}$ cells (Fig S1, B). Human ILC2s isolated from peripheral blood were identified as live $CD45^{+}Lineage^{-}CRTH2^{+}CD127^{+}$cells.

Cell sorting was performed on a FACSAria III cell sorter (BD Biosciences, NJ, USA). Flow cytometry data acquisition was performed on a CytoFLEX (Beckman Coulter, CA, USA).

Apoptosis levels were determined by co-staining of Annexin V (Biolegend, CA, USA) and 7-AAD Viability Staining Solution (eBioscience, CA, USA).

Levels of total ROS were determined using a DCFH-DA probe according to the manufacturer's instructions (Beyotime, Jiangsu, China), and by detection of fluorescent signals on channel 1 by flow cytometry.

Transcriptome Analysis

TRIzol Reagent (Invitrogen, CA, USA) was used to isolate total RNA from ILC2s. Next generation sequencing library was prepared using Ultra RNA Library Prep Kit for Illumina (CA, USA) according to the manufacturer's protocol (New England Biolabs, MA, USA). Sequencing was performed on an Illumina HiSeq instrument following the manufacturer's instructions with a 2 × 150bp paired-end configuration, and the data was analyzed by GENEWIZ (Jiangsu, China). Genes enrichment analysis

based on KEGG pathways was performed on DAVID 6.8 (https://david.ncifcrf.gov/).

Electron Microscopy

ILC2s were suspended in fix solution (Servicebio, Hubei, China) on ice for 2-4 hour. After fixation, cell pellet was embeded with 1% agarose, and washed three times in PBS. The cells were subsequently fixed with 1% OsO4 in 0.1 M PBS (pH 7.4) for 2hour at room temperature. OsO4 was then removed, and cell pellet was rinsed in 0.1 M PBS (pH 7.4) for three times. Cells were dehydrated in a gradient ethanol series before infiltrated with acetone (SCRC, Shanghai, China) and EMBed 812 (SPI, PA, USA). After infiltration, samples were embededby baking in a oven at 60 degree for 48 hour before cut into ultrathin sections (60-80 nm) with ultramicrotome Leica UC7 (Leica, Hessen , Germany). Ultrathin sections were contrasted with uranyl acetate and lead citrate, and examined with a HITACHI HT7700 Transmission Electron Microscopy (Tokyo, Japan). The ImageJ software (National Institutes of Health, MD, USA) was used to show mitochondria for counting, and to calculate the area of the cell.

Statistical Analysis

Data analyses were performedby the GraphPad Prism 6.0 software (GraphPad Software, CA, USA). Statistically significant differences were determined by the Student *t* test or One-way ANOVA, where appropriate. P values < 0.05 were considered statistical significance.

SUPPLEMENTARY DISCUSSION

Uncontrolled airway inflammation predisposes the airway to chronic inflammation and subsequent tissue remodeling, resulting in severe asthmatic conditions. ROS has long been proposed to promote airway inflammation, but the underlying mechanisms are not fully understood. In this study, we revealed the role of ROS in the early phase of airway inflammation, when innate immune cells, such as ILC2s, play important roles. We found that ROS levels in ILC2s increased upon cellular activation. The

increased ROS is required for optimal mTOR –dependent metabolic program and functions of ILC2s.

Protein tyrosine phosphatases are important negative regulators of cellular signaling by inhibiting the function of protein tyrosine kinases. Since protein tyrosine phosphatases possess cysteine residues, they are highly reactive to ROS, and therefore could be the link between ROS and the AKT-mTOR signaling in this study. However, the exact molecular target of ROS in ILC2 responsible for triggering downstream AKT-mTOR signaling remains to be determined in future.

On the other hand, the fact that clinical trials using antioxidant therapy in asthma have been largely ineffective so far[1-4] suggests that the precise use of antioxidant agents at the appropriate situation might be the key to the therapeutic effects of antioxidant therapy. In line with this, our study indicates that NAC antioxidant therapy effectively alleviates IL-33 –triggered ILC2 –mediated immune responses and airway inflammations, suggesting that antioxidant therapy might display anti-inflammatory effects in the early phase of airway inflammations, at least by suppressing ILC2 activation. Besides in mouse models, we also observed significant suppressive effects of NAC on human ILC2 functions in vitro. Future studies using humanized mouse models are needed to confirm the therapeutic potential of antioxidant therapy (using NAC or other reducing agents) on human ILC2 –mediated immune responses and airway inflammations in vivo.

SUPPLEMENTARY REFERENCE

1. Fogarty A, Lewis SA, Scrivener SL, Antoniak M, Pacey S, Pringle M, et al. Oral magnesium and vitamin C supplements in asthma: a parallel group randomized placebo-controlled trial. Clinical and experimental allergy : journal of the British Society for Allergy and Clinical Immunology. 2003 Oct;33(10):1355-9.

2. Allam MF, Lucane RA. Selenium supplementation for asthma. The Cochrane database of systematic reviews. 2004 (2):CD003538.

3. Fogarty A, Lewis SA, Scrivener SL, Antoniak M, Pacey S, Pringle M, et al. Corticosteroid sparing effects of vitamin C and magnesium in asthma: a randomised trial. Respiratory medicine. 2006 Jan;100(1):174-9.

4. Shaheen SO, Newson RB, Rayman MP, Wong AP, Tumilty MK, Phillips JM, et al. Randomised, double blind, placebo-controlled trial of selenium supplementation in adult asthma. Thorax. 2007 Jun;62(6):483-90.

SUPPLEMENTARY FIGURE LEGENDS

Figure S1. Gating strategies for ILC2s and eosinophils. (A) ILC2s were gated as live $CD45^+Lineage^-ST2^+CD90^+KLRG1^+$ single cells, and (B) eosinophils were gated as live $CD45^+Gr\text{-}1^+CD11b^+CD11c^-CD170^+$ single cells, from total liver lymphocytes as examples.

Figure S2. NOX2 is required for IL-33 –driven airway ILC2 responses and inflammation. (A) ROS levels in BALF ILC2s from IL-33 –challenged wild-type or *Nox2*$^{-/-}$ mice. (B) Lung ILC2s from untreated Wild-type or *Nox2*$^{-/-}$ mice were analyzed. (left) Representative graphs of Lin^-ST2^+ cells among live $CD45^+$ lymphocytes in the lung tissue. (right) Absolute numbers of ILC2s per gram lung tissue. (C-E) Wild-type or *Nox2*$^{-/-}$ mice were intranasally administered with IL-33 for 4 days to induce airway inflammation for BALF analysis. (C) (left) Representative graphs of Lin^-ST2^+ cells among live $CD45^+$ lymphocytes in the BALF. (right) Absolute numbers of ILC2s in the BALF. (D) IL-5 and IL-13 levels in the BALF. (E) (left) Representative graphs of SSC^{hi}Siglec-F^+ cells among live $CD45^+$ lymphocytes in the BALF. (right) Absolute numbers of eosinophils in the BALF. (A-E) Data are representative of at least two independent experiments, and are presented as the mean ± SEM (n = 6, unless specified otherwise). *$p<0.05$, **$p<0.005$, ***$p<0.001$.

Figure S3. NAC suppressed cytokine production and proliferation of ILC2 in vitro. (A&B) Mouse ILC2s were pretreated with NAC or equal volume of PBS for 2 hour,

before stimulation with IL-33 for 2 days. Percentages of IL-5, IL-13 (A) or Ki67 (B) –producing ILC2s were shown. (A&B) Data are representative of at least two independent experiments, and are presented as the mean ± SEM (n = 3). *p<0.05, ***p<0.001.

Figure S4. Mitochondria in ILC2s. (A&B) Mouse ILC2s were pretreated with NAC or equal volume of PBS for 2 hour, before stimulation with IL-33 for 2 days. (A) Representative electron microscopy photos of ILC2s. Mitochondria were indicated by arrows. Bars represent 10 μm. (B) Mitochondria numbers per cell were shown (left). Cellular sizes were shown as the area the cell occupied in the photo (right). Data are based on over 10 randomly taken photos. Data are presented as the mean ± SEM. *p<0.05.

Figure S5. NAC alleviated IL-33 –driven airway ILC2 responses and inflammation in *Rag1*$^{-/-}$ mice. (A-C)*Rag1*$^{-/-}$ mice were intranasally administered with IL-33 for 4 days to induce airway inflammation. NAC/PBS was i.p. injected every day. (A) Representative graphs of Lin^{-}ST2^{+} cells among live CD45^{+} lymphocytes, and absolute ILC2 numbers in the BALF were shown. (B) IL-5 and IL-13 levels in the BALF were shown. (C) Representative graphs of SSC^{hi}Siglec-F^{+} cells among live CD45^{+} cells, and absolute eosinophil numbers in the BALF were shown. (A-C) Data are representative of at least two independent experiments, and are presented as the mean ± SEM (n = 6). *p<0.05, ***p<0.001.

Figure S6. Both Rapamycin and NAC alleviated IL-33 –driven ILC2 responses and eosinophilia in the liver. (A-L) B6 wild-type mice (A-C, F-J) or *Rag1*$^{-/-}$ mice (D, E, K, L) were hydrodynamically injected with a IL-33 –encoding plasmid to induce ILC2 infiltration into the liver. Rapamycin/DMSO (A-E) or NAC/PBS (F-L) was i.p. injected every day. (A, D, H, K) Representative graphs of Lin^{-}ST2^{+} cells among live CD45^{+} lymphocytes, and absolute ILC2 numbers per gram liver tissue were shown. (B) Percentages of IL-5 or IL-13 –producing liver ILC2s were shown. (C, E, J, L)

241 Representative graphs of $SSC^{hi}Siglec\text{-}F^{+}$ cells among live $CD45^{+}$ cells in the liver,
242 and absolute eosinophil numbers per gram liver tissue were shown. (F) ROS levels in
243 liver ILC2s were detected. (G) Mean fluorescent intensity of CD69, CD71, and CD98
244 expression on liver ILC2s was determined. (A-L) Data are representative of at least
245 two independent experiments, and are presented as the mean ± SEM (n = 6). *$p<0.05$,
246 **$p<0.005$, ***$p<0.001$.
247

Figure S1

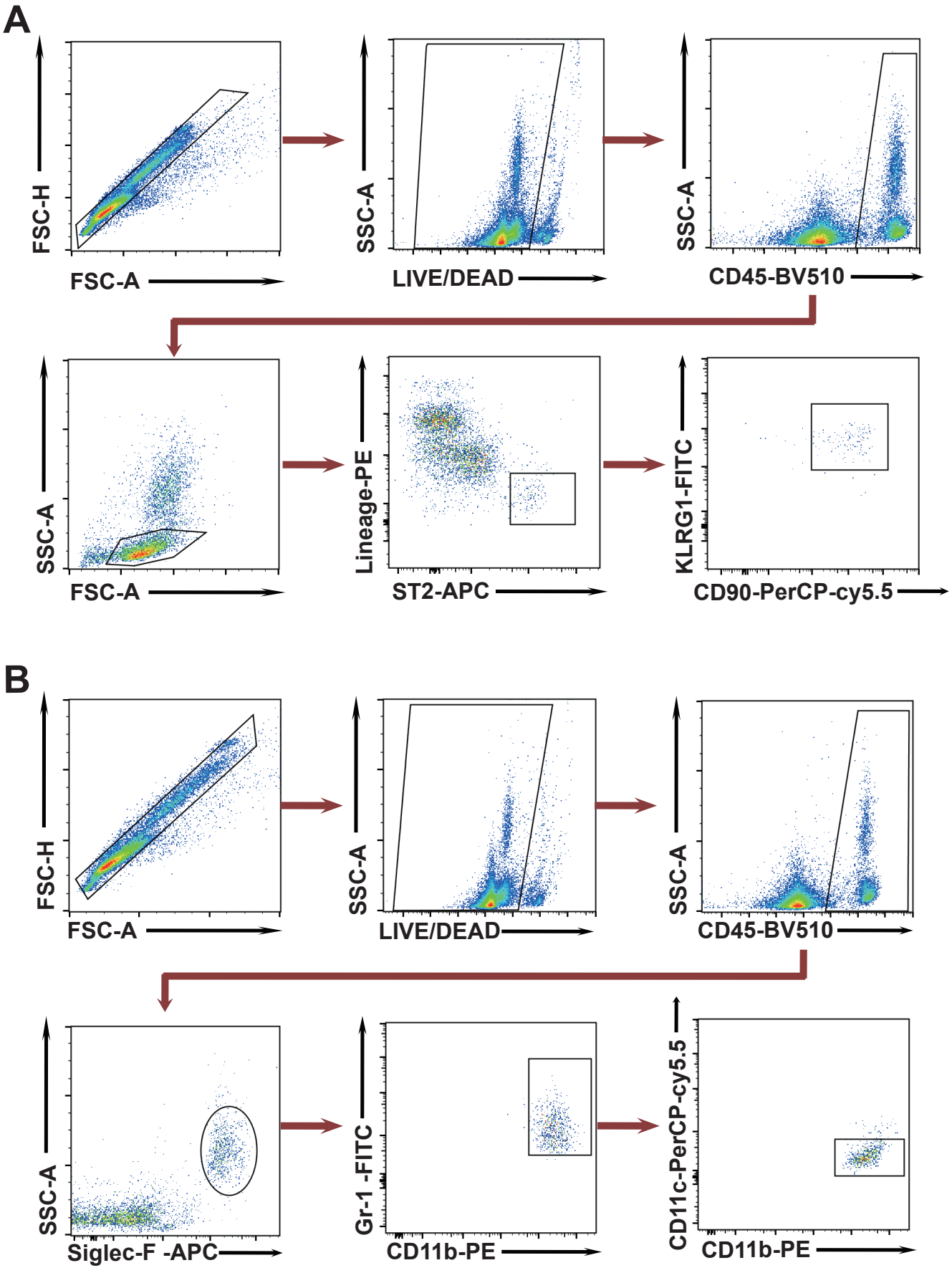
A
FSC-H
FSC-A
SSC-A
LIVE/DEAD
SSC-A
CD45-BV510
SSC-A
FSC-A
Lineage-PE
ST2-APC
KLRG1-FITC
CD90-PerCP-cy5.5
B
FSC-H
FSC-A
SSC-A
LIVE/DEAD
SSC-A
CD45-BV510
SSC-A
Siglec-F -APC
Gr-1 -FITC
CD11b-PE
CD11c-PerCP-cy5.5
CD11b-PE

Figure S2

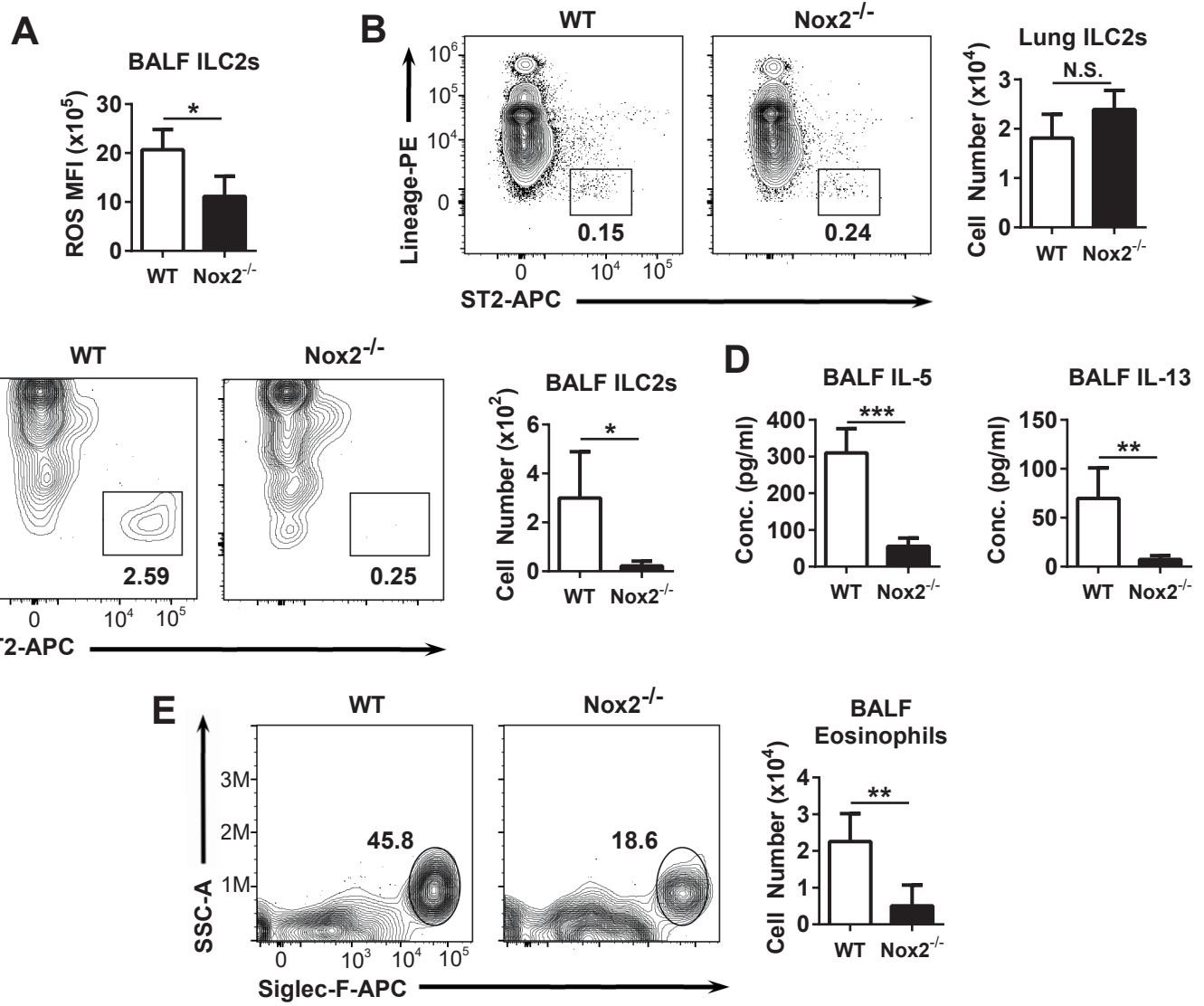
A
BALF ILC2s
ROS MFI (x10^5)
30
20
10
0
*
WT
Nox2-/-
B
WT
Nox2-/-
Lineage-PE
10^6
10^5
10^4
0
0.15
0.24
0
10^4
10^5
ST2-APC
Lung ILC2s
N.S.
Cell Number (x10^4)
3
2
1
0
WT
Nox2-/-
C
WT
Nox2-/-
Lineage-PE
10^6
10^5
10^4
0
2.59
0.25
0
10^4
10^5
ST2-APC
BALF ILC2s
Cell Number (x10^2)
6
4
2
0
*
WT
Nox2-/-
D
BALF IL-5
Conc. (pg/ml)
400
300
200
100
0
***
WT
Nox2-/-
BALF IL-13
Conc. (pg/ml)
150
100
50
0
**
WT
Nox2-/-
E
WT
Nox2-/-
SSC-A
3M
2M
1M
45.8
18.6
0
10^3
10^4
10^5
Siglec-F-APC
BALF
Eosinophils
Cell Number (x10^4)
4
3
2
1
0
**
WT
Nox2-/-

Figure S3

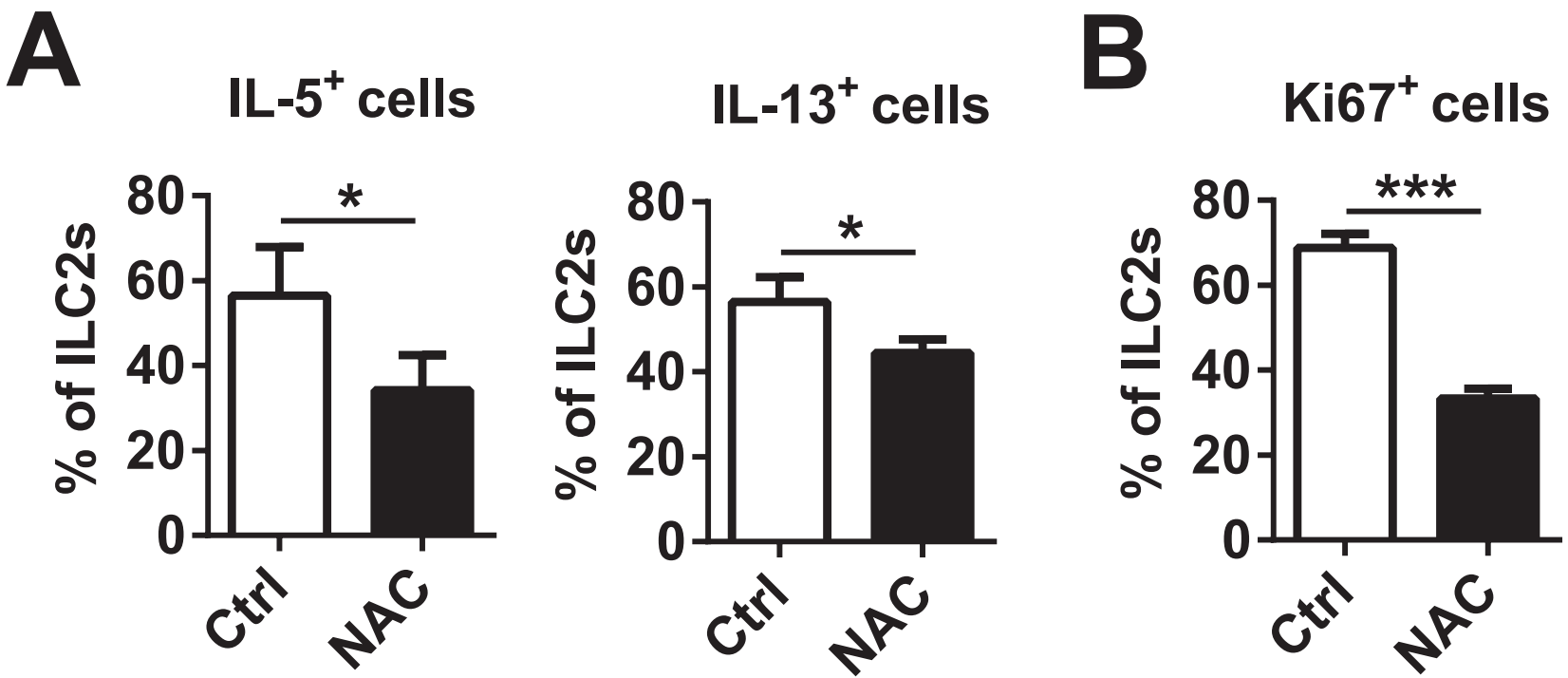
A
IL-5+ cells
% of ILC2s
80
60
40
20
0
*
Ctrl
NAC
IL-13+ cells
% of ILC2s
80
60
40
20
0
*
Ctrl
NAC
B
Ki67+ cells
% of ILC2s
80
60
40
20
0
***
Ctrl
NAC

Figure S4

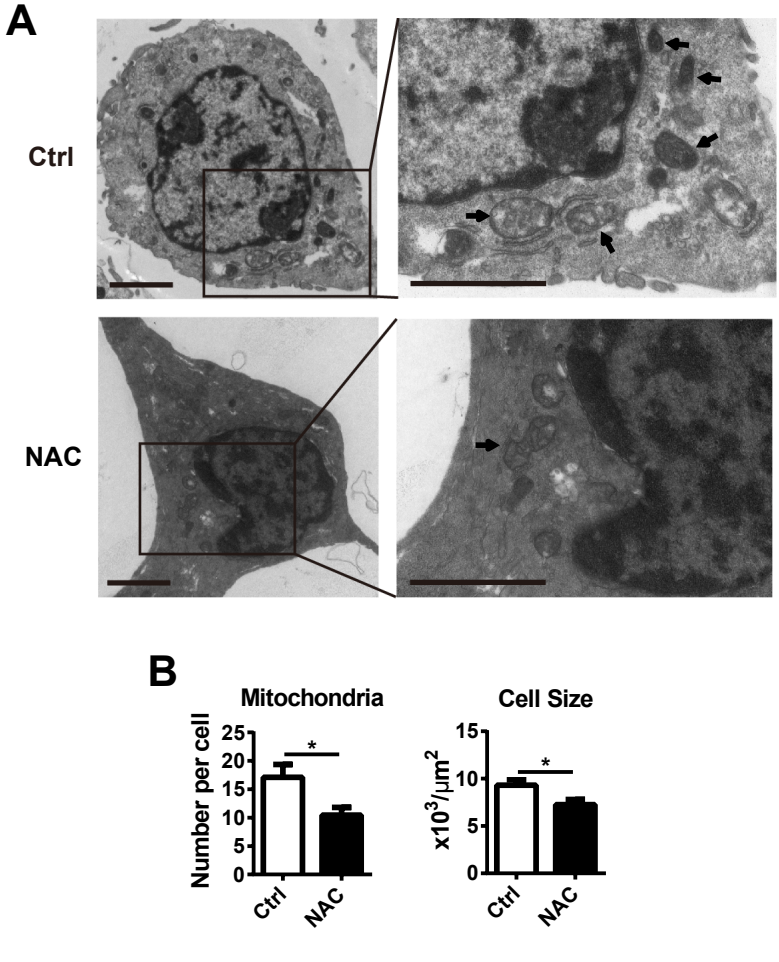
A
Ctrl
NAC
B
Mitochondria
Number per cell
25
20
15
10
5
0
*
Ctrl
NAC
Cell Size
x10^3/μm^2
15
10
5
0
*
Ctrl
NAC

Figure S5

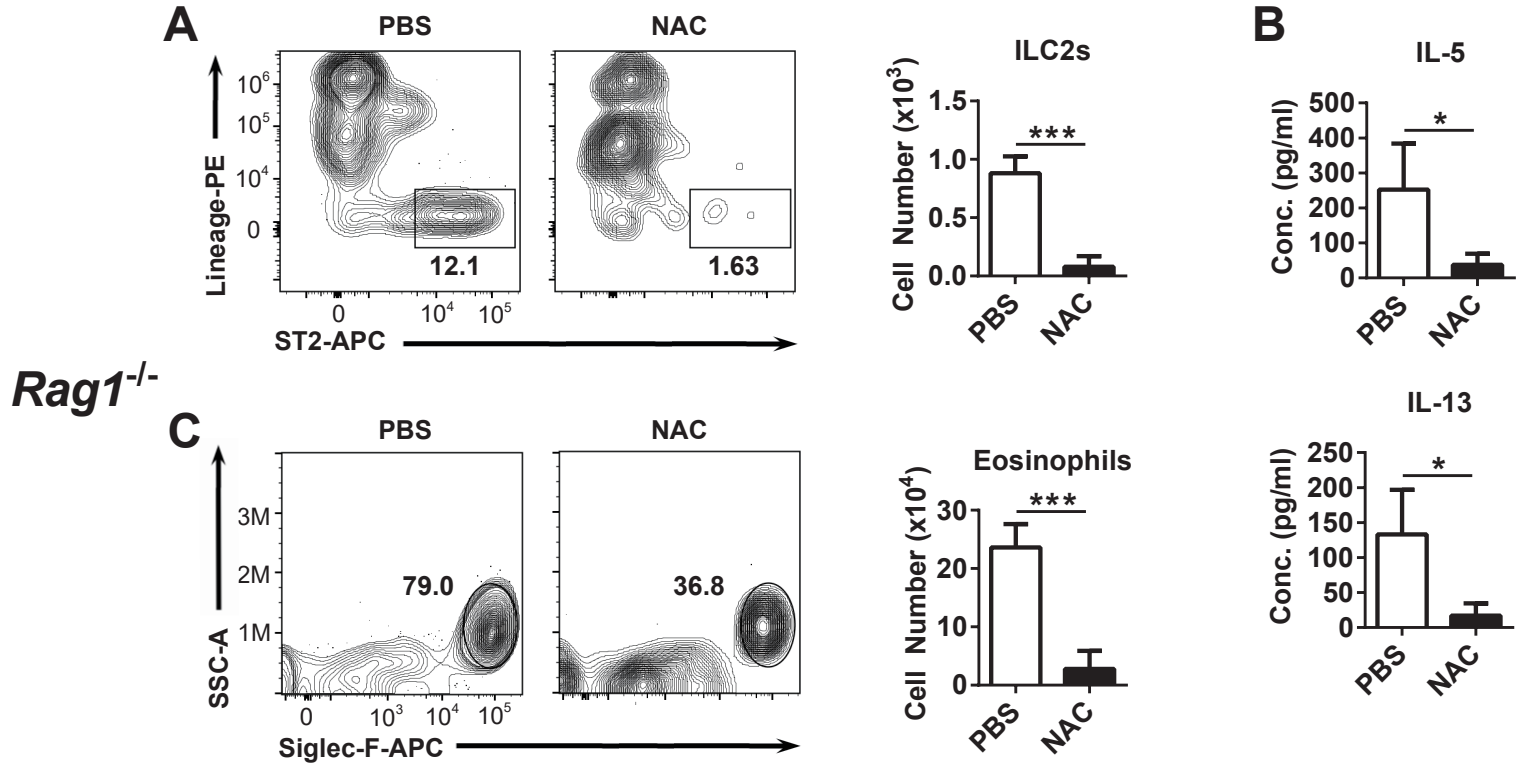
A
PBS
NAC
Lineage-PE
ST2-APC
12.1
1.63
ILC2s
Cell Number (x10^3)
***
PBS
NAC
B
IL-5
Conc. (pg/ml)
*
PBS
NAC
Rag1-/-
C
PBS
NAC
SSC-A
Siglec-F-APC
79.0
36.8
Eosinophils
Cell Number (x10^4)
***
PBS
NAC
IL-13
Conc. (pg/ml)
*
PBS
NAC

Figure S6

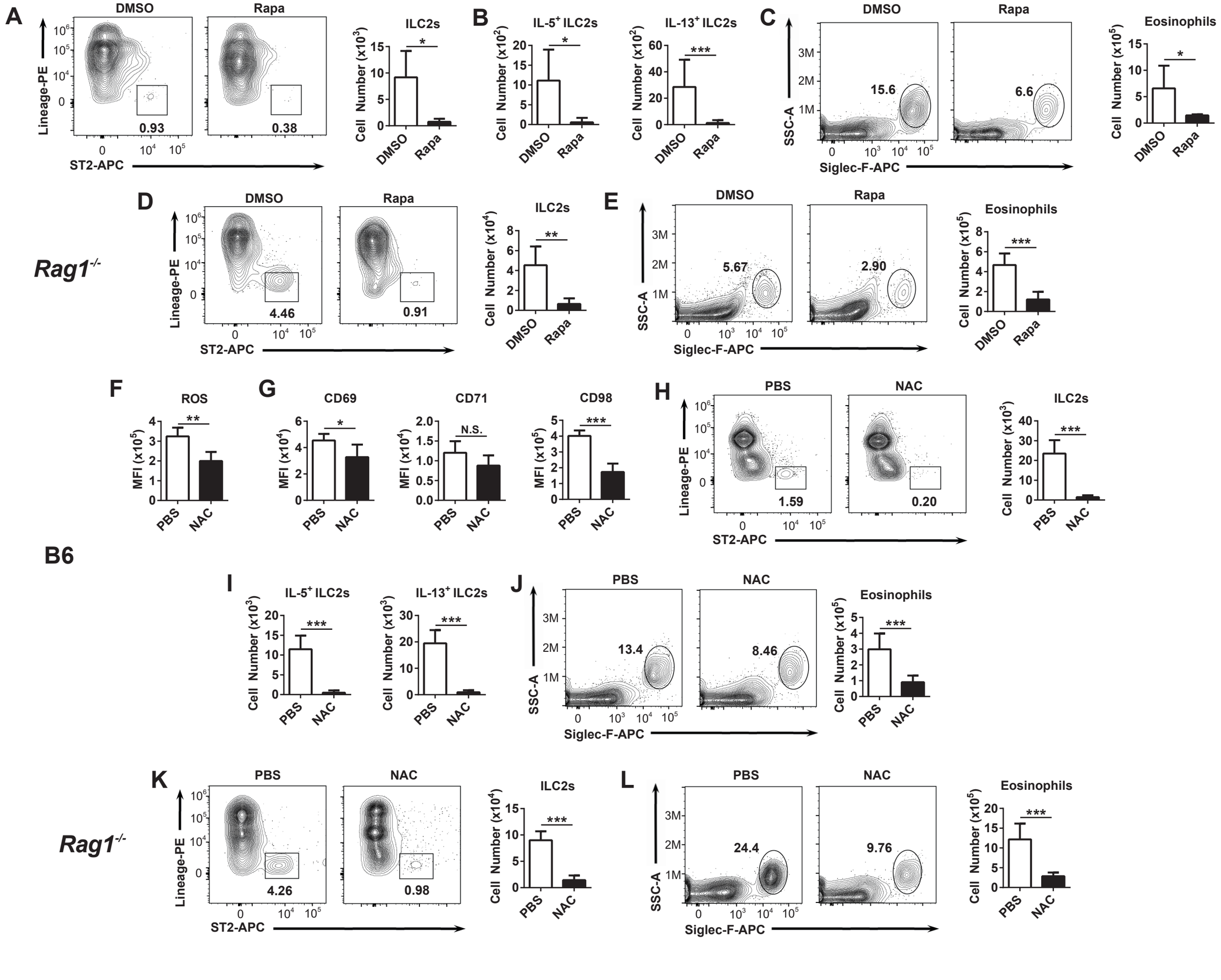
A
B6
DMSO
Rapa
Lineage-PE
ST2-APC
0.93
0.38
ILC2s
Cell Number (x10^3)
B
IL-5+ ILC2s
IL-13+ ILC2s
Cell Number (x10^2)
C
SSC-A
Siglec-F-APC
15.6
6.6
Eosinophils
Cell Number (x10^5)
Rag1-/-
D
4.46
0.91
Cell Number (x10^4)
E
5.67
2.90
F
ROS
MFI (x10^5)
G
CD69
MFI (x10^4)
CD71
N.S.
CD98
MFI (x10^5)
H
PBS
NAC
1.59
0.20
ILC2s
Cell Number (x10^3)
I
IL-5+ ILC2s
IL-13+ ILC2s
Cell Number (x10^3)
J
13.4
8.46
Eosinophils
Cell Number (x10^5)
K
4.26
0.98
ILC2s
Cell Number (x10^4)
L
24.4
9.76
Eosinophils
Cell Number (x10^5)